https://doi.org/10.1016/j.compositesb.2016.04.016

Fabrication and Process Investigation of Vancomycin Loaded Silica Xerogel/polymer Core-shell Composite Nanoparticles for Drug Delivery

[1]W.F. Huang, *[1]Gary C.P. Tsui, [1]C.Y. Tang, [2]M. Yang

[1]Department of Industrial and Systems Engineering, The Hong Kong Polytechnic University, Hung Hom, Kowloon, Hong Kong, China
Interdisciplinary Division of Biomedical Engineering, The Hong Kong Polytechnic University, Hung Hom, Kowloon, Hong Kong, China
*Corresponding author: E-mail address: mfgary@polyu.edu.hk

Abstract

Biodegradable polymer-inorganic composites particles can provide significant advantages while avoiding the shortcomings of using polymer or inorganic particles alone as drug delivery vehicles. Most of the existing fabrication methods for polymer nanoparticles and silica xerogel nanoparticles are not applicable for composite nanoparticles. To overcome these difficulties, a novel sol-gel emulsion polymerization method was successfully developed through the integration of sol-gel and modified double emulsion processes, in which gelation of the silica solution was enabled in nanodroplets generated in the modified emulsion process. Spherical vancomycin loaded silica xerogel/polymer core-shell composite nanoparticles with tunable size and good drug encapsulation efficiency were fabricated through this novel method. By changing the process variables of the modified double emulsion process in terms of sonication time and PVA concentration, the average diameter of the composite nanoparticles could be adjusted in the range of 192~569 nm, with a maximum encapsulation efficiency up to

82.2%. With the introduction of silica xerogel as the primary core material by the sol-gel process, the prepared composite nanoparticles exhibited two times higher encapsulation efficiency, one time lower initial drug release and slower drug release rate than the polymer nanoparticles, enabling these composite nanoparticles to be better candidates for long-term sustained drug release applications.

Keywords: A. Polymer-matrix composites (PMCs); A. Nano-structures; A. Particle-reinforcement; Sol-Gel; Silica xerogel; Drug delivery

1. Introduction

Controlled release systems are gradually becoming an attractive approach for drug delivery, because of their significant advantages over conventional drug delivery systems. Controlled drug delivery systems are designed to deliver drug molecules to particular disease sites and release the drug in a predetermined manner; therefore, they allow outstanding therapeutic efficiency with minimized side effects[1, 2]. With the rapid advances in nanotechnology, nanoparticles have gradually become the most promising vehicles for controlled drug delivery. Not only because of their capability to protect and deliver therapeutics in a manipulated manner, but also a nanoparticulated delivery system is characterized by its capability to penetrate into a deep tissue for cellular uptake known as the enhanced permeability and retention (EPR) effect [2, 3]. According to various fenestration size of organs or pathological situations, the size

requirements of nanoparticulated delivery systems range from several to hundreds of nanometers for different medical treatments [4].

Most nanoparticles developed for drug release are primarily composed of biodegradable polymers, proteins or lipids, leading to excellent degradability, biocompatibility and flexibility. Development of nanocomposite are enormous in recent years[5-10]. However, compared with these organic nanoparticles, very few inorganic nanoparticles, typically ceramics, have been developed for a controlled drug delivery system due to their unfavorable non-degradability and high processing temperature (typically >1000℃), despite their intrinsic advantages over these organic compounds such as higher chemical, thermal and electrical stability, better mechanical properties as well as excellent biocompatibility[7, 11-13].

Although this is the case, the limitations of the inorganic delivery system have been overcome by applying a solution-gelation (sol-gel) technology. Silica xerogel, an amorphous and highly porous silica (SiO_2) form prepared by the sol-gel technology, has been recently considered as an advantageous and promising bioactive inorganic system for controlled drug delivery, due to its good biodegradability, biocompatibility and the mild processing conditions [14-16]. Moreover, the physical properties of silica xerogel, including its density, pore size and internal structure, can be easily manipulated by

controlling the parameters of the sol-gel chemistry. For instance, the pore size of silica xerogel matrix can be reduced by simply switching the catalysis from a base to an acid. Similarly, the drug release rate of silica xerogel can be well controlled by tailoring its structure through adjusting its synthesis parameters such as water/alkoxide ratio, aging time, drying time etc. [4, 5]. Precision control on its properties makes it more advantageous than other drug carriers, such as biodegradable polymers. A variety of active molecules, such as proteins, hormones, antibiotics, anti-cancer agents etc., have been successfully encapsulated by silica xerogel mostly in the form of films or microparticles [17, 18]. Silica nanoparticles were developed by Barbe et al [19, 20] for drug delivery purpose through an emulsion polymerization method combining the sol-gel technology and water-in-oil (W/O) emulsion. This method allows the preparation of desired silica nanoparticles under a low processing temperature, but the process was quite time-consuming and complicated. As compared with polymeric carriers, drug encapsulation efficiency of silica xerogel matrix was much higher due to its porous structure that is capable to efficiently entrap drug molecules [21]. Silica xerogel particles, prepared by the sol-gel based method, were capable of completely encapsulating small molecule drugs, such vancomycin and bupivacaine[17]. However, the encapsulation efficiency of vancomycin loaded polymeric nanoparticles, fabricated by the modified double emulsion technique, was far from complete due to drug leakage during the emulsion process[22-24].

Drug releases from the silica matrix are mainly through the processes of diffusion and dissolution. It has been reported that the silica matrix prepared by the sol-gel method was found to cause no abnormal inflammation or adverse reaction in an animal model, and was capable of dissolving and being excreted through the kidneys in the form of urine, which confirmed the biodegradability and biocompatibility of this material [20, 21]. Despite of all the benefits described above, the silica xerogel matrix has also been discovered to have a high initial burst release due to its porous structure, which therefore limits its application in long term sustained drug release. Some attempts have been made to overcome this limitation by combining the silica xerogel with biopolymers [25-27]. A core-shell nanocomposite was fabricated by coating the drug loaded mesoporous silica with a photo-responsive copolymer in order to control the drug release with the help of the polymeric shell [26]. The silica xerogel core-polymer shell composite micro particles were fabricated by attaching the polymeric nanoparticles to the surface of drug loaded silica aerogel [27]. Release profiles of these composite microparticles could also be well manipulated. Composite films of polymer-silica xerogel were successfully fabricated by Costache et al. [28] through a method of grinding drug loaded silica xerogel in the form of microparticles and then mixing them with a polymer solution. Tensile moduli of these nanocomposites were found to far outweigh those of the unfilled biopolymer, because of the interfacial hydrogen bonding between the polymer and silica xerogel. A significant reduction of the initial drug burst release for the nanocomposite film was also found [28]. Despite the benefits of

combining the silica xerogel and biopolymer as drug delivery vehicles, very few investigations have focused on polymer-silica xerogel composite nanoparticles. This is because most of the methods, which were designed solely for the fabrication of polymeric nanoparticles and silica xerogel nanoparticles, are not applicable for the fabrication of composite nanoparticles [29, 30]. Therefore, it would be clearly worthwhile to develop a facile method for fabricating polymer-silica xerogel composite nanoparticles with desired properties, for application as a drug delivery vehicle.

In order to take the advantages of the biopolymers and silica xerogel carriers, as well as overcoming their shortcomings, the present study was initiated to develop a novel sol-gel emulsion polymerization method to fabricate drug loaded silica xerogel/polymer core-shell nanoparticles with high encapsulation efficiency, tunable submicron size, low initial drug release and long sustained release profiles. Vancomcin HCl, selected as a drug model, is a glycopeptide, an antibiotic used in the treatment of life-threatening infections caused by Gram-positive bacteria. The biodegradable polymer, Poly (L-lactide) (PLA), approved by the FDA, was adopted as the primary component of the polymeric shell. Moreover, another biodegradable polymer, PLGA-mPEG was used for stabilizing the emulsion as well as enhancing the dispensability and circulation of the prepared nanoparticles due to the existence of a PEG block in the polymer chain. The effects of different processing variables on drug encapsulation efficiency and the size of the prepared nanoparticles were explored and discussed. A short term drug release study

was also conducted for verification of the performance of the fabricated composite nanoparticles.

2. Material and methods

2.1 Materials

Poly (L-lactide) (PLA) (Mw: 2 kDa), PLGA-PEG (Mw: 1.1 kDa) was obtained from the Jinan Daigang Biomaterial Co., Ltd. Dichloromethane (DCM), HCl, Alcohol and NH4OH were purchased from the Merck & Co. Polyvinyl alcohol (PVA) (Mw: 2.3 kDa), Tetraethylorthosilicate (TEOS) was acquired from the Sigma-Aldrich. Vancomycin HCl (VC) was obtained from Biofer and used as a drug model for the present study.

2.2 Synthesis of drug loaded Silica Xerogel/polymer Composite Nanoparticles

An overview of fabrication method for the silica xerogel/polymer composite nanoparticles in micro-carriers is depicted in Fig.1. Typically, 11 ml TEOS, 17.7ml H_2O and 0.2 ml 1 mol/L HCl solution were mixed under agitation at room temperature until TEOS was completely hydrolyzed and a clear sol-gel solution was formed. 15 mg of vanconmycin HCl (VC) and 0.05 ml of 1% NH_4OH solution was mixed and then dissolved in 1 ml of the as-prepared sol-gel solution as the core material of the composite nanoparticle. This sol-gel drug solution, as an internal phase, was then

ultrasonically homogenized for 3 minutes using an ultrasonic cell crusher (Model SKL250-11N, Ningbo Haishu Sklon Electronic Instrument Co. Ltd) into 10 ml of polymer solution (shell material) to obtain the primary emulsion. During preparation of the primary emulsion, 0.25 ml of 1% NH_3 solution was gradually added to initiate gelation of the sol-gel drug solution. The polymer solution was prepared by dissolving 3 g of PLA and 0.2 g of mPEG-PLGA into 10 ml of DCM. The primary emulsion was then dispersed into a PVA aqueous solution with a concentration in the range of 0~2.5% under sonication for 0.5-3.5minutes, to generate a secondary emulsion. A suspension of VC loaded silica xerogel/polymer nanoparticles was obtained after 3-hour mild agitation to eliminate DCM at room temperature. The nanoparticles suspension was centrifuged at 12000 rpm using a high-speed centrifuger (Model TG16-W, Hunan Xiangyi Centrifuge Instrument Co., Ltd) for 30 minutes and the supernatant was kept for drug concentration analysis by using UV/vis spectrophotometry (Model UV1102, Techcomp Ltd). The final drug loaded silica xerogel/polymer composite nanoparticles were obtained after washing, filtering and drying.

2.3 Synthesis of Drug Loaded PLA nanoparticles

For better comparison, drug loaded PLA nanoparticles were also prepared by using a double emulsion method. Briefly, 15 mg of VC was dissolved in 1ml of pure water to form a drug solution. This drug solution was then emulsified into 10 ml of polymer

solution containing 0.5g of PLA and 10 ml of DCM under sonication to form the primary emulsion. This emulsion was then dispersed into 1.5% PVA aqueous solution under 2-minute sonication to obtain a secondary emulsion. A suspension of polymer nanoparticles was obtained after the DCM was evaporated under 3-hour mild agitation at room temperature. The suspension of the nanoparticles was then centrifuged at 12000 rpm using high-speed centrifuge for 30 minutes and the supernatant was kept for drug concentration analysis by UV/vis spectrophotometry. The final drug loaded PLA nanoparticles were obtained after washing and drying.

2.4 Characterization

The morphology and structure of the samples were observed by using field emission electron microscopy (TEM) (JEOL Model JEM-2100F) and scanning electron microscopy (SEM) (JEOL JSM-6490). Specimens for TEM were prepared by dissolving the micro-carriers in pure water and dropping the suspension of nanoparticles onto carbon-coated copper grids for solvent evaporation. Compositional information on the nanoparticles was confirmed by Fourier Transform Infrared (FTIR) spectrometry (Spectrum 100T, PerkinElmer). Thermal properties of the samples and raw materials were studied by using a thermogravimetric analyzer/differential scanning calorimeter (TGA/DSC) (Netzch STA 449C, Jupiter) at a heating rate of $10℃min^{-1}$, from 50 to 450℃. The average size of the nanoparticles was determined by a Zetasizer Nano ZS (Malvern Instruments, Malvern, U.K.) instrument.

2.5 Determination of Drug Loading and Encapsulation Efficiency

The concentration of the vancomycin in the supernatant was identified by measuring its absorbance by using UV spectrophotometry at 280.5 nm. A standard curve, that was used to calibrate the relationship between the drug concentration and UV absorbance, was prepared using a drug concentration in the range of 0.6 ~ 0.032 mg/ml in 1.5% of PVA. It had a regression equation of $y = 0.2347x+0.00942$, with a correlation factor R of R=0.996. The encapsulation efficiency (EE) of the vancomycin in nanoparticles was determined by identifying the concentration of the non-encapsulated free drug in the supernatant after centrifugation of the nanoparticle suspension at 12000 rpm for 30 minutes.

The EE of the drug loaded nanoparticles was calculated by using the following equation:

$$\text{Encapsulation Efficiency (\%)} = \frac{\text{Total drug amount} - \text{Free drug amount}}{\text{Total drug amount}} \times 100\%$$

2.6 In Vitro drug release

An appropriate amount of nanoparticles containing 11 mg of vancomycin was dispersed into 100 ml of PBS solution （pH = 7.3 ± 0.1）in a 150 ml flask with a cap. The flasks were shaken at 100 cycles/min in a gas bath shaker at a temperature of 37.0±0.2℃. 4 ml of dissolution medium was withdrawn from each flask and kept for further processing,

while 4 ml of fresh PBS solution were added to the flask at fixed time intervals. Before taking the dissolution medium, agitation ceased for 15 minutes to allow for the precipitation of the nanoparticles. The collected dissolution medium samples were subjected to centrifugation at 12000 rpm for 5 minutes and the corresponding supernatant was kept for drug concentration analysis using UV/vis spectrophotometry at 280.5 nm.

3. Results and Discussion

3.1 Size, morphology and structure of nanoparticles

The average size (diameters) of the prepared composite nanoparticles with different process parameters ranged from 192 to 569 nm with polydisperse index (PDI) ranging from 0.180 to 0.578. The size and PDI of the particles were significantly influenced by the sonication time (2^{nd} sonication time) of the second emulsion and PVA concentration. Particles with the greatest PDI (0.578) and radius (569 nm) were prepared with the shortest 2^{nd} sonication time (0.5 minutes) and 0% PVA concentration (Fig.2(b)). The longest 2^{nd} sonication time (3.5 minutes) and 0% PVA concentration lead to the lowest PDI (0.180) and the smallest particle diameters (192 nm)(Fig.2(a)). A detailed explanation is presented in the section 3.5.

As shown in Fig.2 (a), the as-prepared composite nanoparticles exhibits spherical shapes and smooth surfaces. The core-shell structures of the particles are clearly observed in Fig.2 (b)-(d): the dark spots in the middle of the particles are the drug loaded silica xerogel core materials, while relatively light regions are the polymeric shells. Most of entrapped silica xerogel core exhibited spherical shape as shown in Fig2(b). Several non-spherical silica xerogel core, such as triangular and irregular shapes, were also observed in some composite nanoparticles, as shown in Fig.2(c & d). These phenomena can be explained by different gelation rates that were associated with heterogeneous collisions between droplets of Sol-gel drug solution and NH_3 solution in the primary emulsion. The gelation process is characterized by the gradual transformation of sol-gel solution from liquid phase to gel phase accompanying by increasing viscosity. As presented in Fig.3, the time required for sol-gel solution to transform from liquid to gel (gelation time), also known as rate of gelation, is inverse proportional to the concentration of NH_3 in sol-gel solution. According to our fabrication process, NH_3 solution is added during the emulsification of sol-gel drug solution. After the addition of NH_3 solution, sol-gel drug solution and NH_3 solution coexist in the form of nano-droplets in the primary emulsion. Brownian movement induces the collisions of NH_3 and Sol-gel droplets. Collisions occur in the routes as shown in Fig.4. In route 1, two NH_3 droplets collide with one sol-gel droplet, which resulted in immediate formation of gel (high gelation rate) on the beginning of the merging process of these three droplets due to the relative high NH_3 concentration (high

NH_3/Sol-gel ratio). A triangle shape is then formed. In the opposite way, when two sol-gel droplets collide with one NH_3 droplet as shown in route 3, the relative low NH_3 concentration contribute to a reducing gelation rate, which allowed complete merging of three droplets into a larger droplet. Usually, cavitation effect of sonication can cause the fluctuation of this large droplet and will then disintegrate it into smaller droplets. When a gel state was formed during the fluctuation and before the integration, the irregular shape core is generated as shown in Fig. 2(d). When a gel state was formed at the moment when each one NH_3 and Sol gel droplets just merge into large one as shown in route 2, the spherical cores is then formed. These explanations can be supported by the fact that silica xerogel cores of triangle and irregular shapes are similar in size while larger than spherical one. It was discovered that most of the silica xerogel core exhibited spherical shape. Since there are only a small parts of the particles exhibited non-spherical shape core, no significant impacts of these particles of non-spherical shape cores were found.

Cores of Irregular shape that are larger than the one in Fig 2(d) were rarely been found. This can be explained by the balance between cavitation effect of sonication and agglomeration of Nano-droplets. The cavitation effect tends to disintegrate large droplets into smaller ones, which therefore prevents agglomeration/collision of too many droplets. Therefore, route 1&3 occur less frequently than route 2. To prove this assumption, samples prepared with diluted NH_3 concentration (0.6%) were prepared.

The silica xerogel cores of triangle shapes of these samples were rarely discovered under TEM observation.

3.2 Thermal analysis

Differential scanning calorimeter (DSC) analysis curves of PLA, a mixture of all the raw materials of drug loaded composite nanoparticles, drug free composite nanoparticles (composite nanoparticle without addition of drugs during fabrication) and drug loaded composite nanoparticles are shown in Fig.5. The endothermic peaks at 169℃ are the characteristic of the melting behavior of PLA. The exothermic peaks of the drug free and drug loaded composite nanoparticles at correspondingly 106℃ and 113℃ represent the cold crystallization behavior of PLA, which is assumed to have been caused by the solvent evaporation step in the fabrication process of the composite nanoparticles. When the solvent in the solution gradually evaporates, the concentration of the polymer solution increase and the interactions between the polymer molecular chains are induced in the concentrated polymer solution, due to the uncomplete crystallization of PLA [31, 32]. For the thermal analysis, the crystallization process continued, because the temperature of PLA was elevated to particular values, such as 106℃ and 113℃ in this study. It is discovered that the cold crystallization temperature of the drug loaded composite nanoparticles is higher than that of drug free particles. This suggests that encapsulation of the drug could reduce the mobility of PLA chains and thus hinders its crystal growth. The characteristic peak for cold crystallization is not

observed from the DSC curves of PLA and the mixture of raw materials, which proved the correctness of the assumption that the uncompleted crystallization of PLA occurred in the fabrication process. Unlike the drug free composite nanoparticles, there are small endothermic peak and exothermic peak at 233℃and 285℃ for the DSC curve of the drug loaded composite nanoparticles. The endothermic peak at 233℃ is attributed to the decomposition behavior of the loaded drug, while the exothermic peak at 285℃ may be ascribed to the potential reactions between the drugs and PLA, such as the dehydration condensation reaction between -NH_2 groups of drugs and –COOH groups of PLA. A endothermic peak at 71℃ is observed on both drug loaded composite nanoparticles and the mixtures of all raw materials, which may result from the esterification reactions between the –OH groups of silica xerogel and –COOH groups of the drug (Vancomycin HCl) in alkaline environment. This endothermic peak of the mixture was more significant, because the raw materials were not mixed in the same ratio as composite nanoparticles. When the mixture is prepared by mixing all the raw materials with the same ratio as composite nanoparticles, this endothermic peak is much less significant. The differences of the curves after 300℃ are the results of their inhomogeneous and irregular decomposition behaviors of the samples.

3.3 FT-IR analysis

The qualitative composition of composite nanoparticles was investigated by FT-IR spectroscopy, as shown in Fig.6. FT-IR spectra of composite nanoparticles is similar

with PLA and polymer nanoparticles in most parts, which indicates PLA as one of the compositions of composite nanoparticles. The strong absorption peak observed at 1755 cm^{-1} is attributed to the stretching vibration of the carbonyl groups (C=O), which are the representative bonds of PLA and PLGA-mPEG. The absorption peaks at 3003 and 2955cm^{-1} correspond to asymmetric and symmetric stretching vibration of the C-H bonds of $–CH_3$ groups of PLA and PLGA-mPEG. The peak at 565 cm^{-1} may result from the bending vibrations of C-C=O groups of PLGA-mPEG, which proves the existence of PLGA-mPEG in composite nanoparticles. Characteristic absorption peak at 465 cm^{-1} corresponds to the bending vibration of Si-O-Si bonds, which is the evidence of silica xerogel in composite nanoparticles. The peak at 2975 cm^{-1} of TEOS curve is owing to the asymmetric stretching vibration of the C-H bonds of $–CH_3$ groups. The absence of this characteristic absorption peak of $–CH_3$ groups in the spectra of silica indicates that the TEOS has been hydrolyzed completely during the preparation of silica xerogel. The peak at 3486 cm^{-1} of silica is associated with H-bonded Si-OH stretching vibrations and H-bonded water. The existence of –OH groups also indicate a hydrophilic surface of the silica xerogel core that enabled the water soluble drug to accumulate on the surface. More detailed discussion on this can be found in section 3.7.

3.4 Effect of PVA concentration

It was surprising to discover in our study that an increase of PVA concentration caused increasing size and reducing EE of the nanoparticles (Fig.7) under the current

formulation rather than a reduction as found in most investigations discussed above. These phenomena are due to the results of competing effects of the addition of PVA into aqueous solution. This competing effects were rarely discussed and compared in publications. As summarized in table 1, PVA acts as 3 roles simultaneously in aqueous solution. Each of these roles can lead to an independent effect on EE and size of the composite nanoparticles. The relationships between PVA concentration and EE/size of composite nanoparticles are the combination effects of these roles.

As an emulsifier, increasing PVA contributes to reduction of the surface tension of solution and thus lead to easy breakdown or fragmentation of large droplets in the second emulsion, which therefore lead to decreased particle size[33]. The fragmentation of large droplets will also cause the escape of drug from internal phase, because of the exposure of drug to aqueous solution[34]. However, There is a threshold of the concertation of PVA, beyond which a further increase of PVA content will have no significant impact on the size of the nanoparticles[33] As an viscosity enhancer, augmentation of PVA concentration in aqueous solution, as we found, lead to increasing viscosity of aqueous solution, which limits the fragmentation of large droplets of the second emulsion under certain sonication power/time and therefore cause increase of both size and EE. Acting as osmotic pressure solution, PVA solution of large concentration can create osmotic pressure gradient between PVA aqueous solution and drug solution of the core of nanoparticles, while polymer shells acts as the

semipermeable membranes[35]. The outward force caused by osmotic pressure would lead to outflow of free water in the core of nanoparticles through the polymer shell to aqueous solution[36]. This process is more likely to occur during solvent evaporation process, when polymer shells are solidified as the evaporation of organic solvent. Outflow of free water from the core could cause the loss of highly hydrophilic drugs along with water, owing to the attractions between hydrophilic drug molecules and water molecules. This escape of drug molecules is more significant when the molecular weight of hydrophilic drugs is much smaller than that of polymer shells, due to theirs high permeability through polymer shells of long molecule chains[37]. In current case, most of sol-gel drug solution have become gels instead of fluid during the second emulsion process. Aging of these gels occur after gelation, which result in the shrinkage of gel and release of some entrapped water[21]. The escape of water molecules from gel matrix can bring along with hydrophilic drug molecules to the gap between silica xerogel core and polymer shell. The osmotic pressure cause the outflow of these water and drug molecules from composite nanoparticles.

Significance of the influences of these 3 roles on size and EE is assumed to be ranked as: emulsifier & osmotic pressure solution > viscosity enhancer. It should be notified that significance of osmotic pressure solution is less significant or even ignorable when molecular weight of molecules encapsulated are larger than that of polymers used, such as proteins, since large molecules are difficult to permeate through solidified polymer

shell. This is the reason why nanoparticles loaded with proteins (such as bovine serum albumin) usually have higher EE than that loaded with small antibiotic loaded nanoparticles[22, 34]. In most investigations of nanoparticles fabricated by double emulsion based technology as discussed in section 1, size and EE are proportional to PVA concentration. This tendency is consistent with the effects of emulsifier/osmotic pressure solution; while contrary to the effect of viscosity enhancer. These results proved the leading effects of emulsifier/osmotic pressure solution over viscosity enhancer. In the fabrication of proposed composite nanoparticle, amphiphilic polymer PLGA-mPEG and small drugs (Mw:1485 Da) are used. The amphiphilic structure of PLGA-mPEG enable it to possess the surface active property and thus can act as an emulsifier. The existence of PLGA-mPEG make the effect of emulsifier role of PVA much less significant, which make effect of osmotic pressure solution the leading effect in current situation. The change of EE along various PVA concentration presented in Fig.7 is consistent with the effect of osmotic pressure solution; while the trend of size is consistent with the effect of viscosity enhancer. These results prove the correctness of the assumption mentioned previously.

3.5 Effect of the 2nd sonication time

The effects of the 2nd sonication time on size and EE of the composite nanoparticles prepared with the same PVA concentration (1.5%) are shown in Fig.8. This result can be explained by the fact that prolonged ultrasonic treatment resulted in more

fragmentation of droplets and thus led to the formation of finer nanoparticles. This increasing fragmentation effect, however, can induce more drug leakage from silica xerogel by contacting with aqueous solution, which are similar with the effect of emulsifier discussed in section 3.4. The effect of size reduction was gradually mitigated with increasing sonication duration. Size of composite nanoparticle range from 386 nm to 241 nm with adjustment of the 2^{nd} sonication time. The minimum size was reached when the 2^{nd} sonication time was increased to 3.5 min.

Comparing with the adjustment of PVA concentration, increasing the 2^{nd} sonication time is an more effective way to control the mean particle size. However, size reduction by the adjustment of 2^{nd} sonication time needs to be compromised with the drug encapsulation efficiency. In the fabrication of composite nanoparticles, size reduction by changing PVA concentration is beneficial for EE. Viewing the relationship between size and EE, the conclusions drew from PVA and the 2^{nd} sonication time adjustment are contrary. This seeming contradiction attributes to different size reduction mechanisms of the two adjustment routes. According to the discussion in section 3.4, reduction of size and improvement of EE along decreasing PVA concentration are owing to the combination effects of viscosity enhancer and osmotic pressure solution. The reduction of size and EE by increasing sonication time is associated with the fragmentation of droplets, which was similar with the effect of emulsifier as shown in table 1. To prove this conclusion, samples prepared with different sonication time and 0% PVA

concentration were prepared (Fig.8). EE of these samples are higher than that of 1.5% PVA, which is consistent with the assumption made previously about impact of the osmotic pressure solution. Size of the samples prepared with 1.5-3.5 sonication time is smaller than that of the corresponding samples of 1.5% PVA, which also prove the assumption on the effect of viscosity enhancer. Samples prepared with 0.5 sonication time and 0% PVA possess the largest particle size. This situation results from the insufficient emulsification because of too short sonication time and the absence of PVA, which prove effects of PVA as an emulsifier.

3.6 Comparison between polymer and composite nanoparticles

To compare with the similar nanoparticles available in literatures, properties of vancomycin loaded particles prepared with biodegradable polymer are collected in table 2. Since there are few investigations concerning the vancomycin loaded polymer nanoparticles, properties of vancomycin loaded polymer microparticles were also collected. Comparing with similar nanoparticle, the prepared composite nanoparticles possessed much lower burst release rate and better EE. Some vancomycin loaded micro particles had better EE than composite nanoparticles, because less fragmentation occurred during the fabrication of micro particles. However, Burst release of these microparticles, because of the absence of silica xerogel core, were much larger than most of the micro particles. When considering both burst release and EE Simultaneously, composite nanoparticles possess the best performances among those

nano/micro particles. However, the limitation of these absolute comparisons is the fact that differences of the process parameters and conditions that can impact the properties of particles (such as particle size, drug loading, temperature, materials, equipment) are ignored, which therefore make the conclusion less convincing.

To avoid these limitations, vancomycin loaded polymer nanoparticles were prepared with similar conditions as composite nanoparticles for better comparison. As shown in table 3, the diameters of the drug loaded composite nanoparticles are similar to those of the polymer nanoparticles, but larger than those of the drug free composite nanoparticles because of addition of the drugs. The EE of the drug loaded composite nanoparticles (71.8%) is much higher than that of drug loaded polymer nanoparticles (34%). 24 hours drug burst release of composite nanoparticles (50%) is much less than polymer nanoparticles (80%), which is discussed in details in section 3.7. The high EE of composite nanoparticles results from the fact that gelation of sol-gel solution can prevent future leakage of the drug in the second emulsion comparing with polymer nanoparticles. Unlike composite nanoparticles, it was found that polymeric nanoparticles cannot be fabricated without the addition of PVA in the 2^{nd} emulsion. Therefore, the fabrication process of the composite nanoparticles can be simplified without the need of an extra step to remove the PVA from the surface of the particles.

3.7 In Vitro drug release studies

The drug release profiles of composite nanoparticles and polymer nanoparticles are shown in Fig.9. A much higher initial release and faster release rate are observed for the polymer nanoparticles (Table 3). For the composite nanoparticles, a lower initial release and slower release rate are found owing to the presence of silica xerogel that limited and deferred the escape of drug molecules from nanoparticles.

As drug molecules are entrapped in the matrix of silica xerogel, drug release from the composite nanoparticles is determined by the erosion of the polymeric shell and silica xerogel core. Therefore, the drug release profile from the composite nanoparticles can be divided into two stages. The first stage was characterized by a relatively fast release rate within 24 hours, which can be attributed to the fact that part of the drug accumulated on the surface of the silica xerogel core and tended to release out through the eroding polymeric shell. The drug accumulation on the interface between the hydrophilic surface of the silica xerogel core and polymeric shell is associated with the aging of silica xerogel and the interactions (such as the hydrogen bond and van de Waal's forces) between water soluble drugs and hydrophilic PEG segments in the polymer shell. These interactions hindered the mobility of the PLA chains and thus lead to a higher cold crystallization temperature, as discovered and discussed in section 3.2. The second stage is characterized by a much slower drug release rate that results from drug release during the slow eroding process of silica xerogel. A complete release of

polymeric nanoparticles was found to occur in 22 days, while it took 66 days to achieve a complete drug release for the composite nanoparticles (Table 3). This low release rate of composite nanoparticles makes them promising candidates for long term drug release application.

4 Conclusions

Vancomycin loaded silica xerogel/polymer core-shell composite nanoparticles were fabricated by a novel method that successfully integrated the modified double emulsion and sol-gel techniques. With the modified double emulsion process, the average diameter of the prepared spherical composite nanoparticles could be freely tuned in the range of 192-569 nm, with maximum drug encapsulation efficiency up to 82.2%, by changing the process variables in terms of the 2^{nd} sonication time and PVA concentration. The tunable size makes composite nanoparticles applicable for broader medical treatments with various size requirements. With the introduction of silica xerogel as the primary core material through the sol-gel method, the prepared composite nanoparticles, as compared with polymeric nanoparticles, possess a double high encapsulation efficiency, one time lower initial drug release (for better controlled drug release applications) and much slower drug release rate (suitable for long-term sustained drug delivery application). Gelation of the silica solution that occurred in the nano-droplets of the second emulsion could effectively prevent drug leakage from the cores of the composite nanoparticles, and thus result in an increase of encapsulation

efficiency. In addition to the degradation of the polymer shells, the drug release from the composite nanoparticles was governed by the erosion of the silica xerogel core, which accounts for the slower release rate of the composite nanoparticles. The amphiphilic structure of PLGA-mPEG enabled the fabrication of composite nanoparticles without the need of adding an emulsifier (PVA) in the second emulsion, which cannot be achieved in the conventional process. This study provides useful information on the development of composite nanoparticles for biomedical applications. For future work, the proposed method will be further extended to broaden the size adjustment window of the composite nanoparticles from tens to hundreds of nanometers, while maintaining good encapsulation efficiency.

ACKNOWLEDGEMENTS

The authors would like to thank the support from the Research Committee of The Hong Kong Polytechnic University (RTE9) for support in this study.

References

Primary Sources

Secondary Sources

Uncategorized References

[1] Deng H, Lei Z. Preparation and characterization of hollow Fe3O4/SiO2@PEG–PLA nanoparticles for drug delivery. Composites Part B: Engineering. 2013;54:194-199.

[2] Danhier F, Ansorena E, Silva JM, Coco R, Le Breton A, Preat V. PLGA-based nanoparticles: an overview of biomedical applications. Journal of controlled release : official journal of the Controlled Release Society. 2012;161:505-522.

[3] Mishra D, Hubenak JR, Mathur AB. Nanoparticle systems as tools to improve drug delivery and therapeutic efficacy. Journal of biomedical materials research Part A. 2013;101:3646-3660.
[4] Gaumet M, Vargas A, Gurny R, Delie F. Nanoparticles for drug delivery: the need for precision in reporting particle size parameters. European journal of pharmaceutics and biopharmaceutics : official journal of Arbeitsgemeinschaft fur Pharmazeutische Verfahrenstechnik eV. 2008;69:1-9.
[5] Yang Q, Liu L, Hui D, Chipara M. Microstructure, electrical conductivity and microwave absorption properties of γ-FeNi decorated carbon nanotube composites. Composites Part B: Engineering. 2016;87:256-262.
[6] Yao Y, Li J, Lu H, Gou J, Hui D. Investigation into hybrid configuration in electrospun nafion/silica nanofiber. Composites Part B: Engineering. 2014;69:478-483.
[7] Yan F, Zhang X, Liu F, Li X, Zhang Z. Adjusting the properties of silicone rubber filled with nanosilica by changing the surface organic groups of nanosilica. Composites Part B: Engineering. 2015;75:47-52.
[8] Wang Y, Liu H, Cheng H, Wang J. Interface engineering of fiber-reinforced all-oxide composites fabricated by the sol-gel method with fugitive pyrolytic carbon coatings. Composites Part B: Engineering. 2015;75:86-94.
[9] Ho MP, Lau KT, Wang H, Hui D. Improvement on the properties of polylactic acid (PLA) using bamboo charcoal particles. Composites Part B: Engineering. 2015;81:14-25.
[10] Lu H, Wang X, Yao Y, Gou J, Hui D, Xu B, et al. Synergistic effect of siloxane modified aluminum nanopowders and carbon fiber on electrothermal efficiency of polymeric shape memory nanocomposite. Composites Part B: Engineering. 2015;80:1-6.
[11] Radin S, Chen T, Ducheyne P. The controlled release of drugs from emulsified, sol gel processed silica microspheres. Biomaterials. 2009;30:850-858.
[12] Najigivi A, Khaloo A, Iraji zad A, Abdul Rashid S. Investigating the effects of using different types of SiO2 nanoparticles on the mechanical properties of binary blended concrete. Composites Part B: Engineering. 2013;54:52-58.
[13] Yadav M, Rhee KY, Park SJ, Hui D. Mechanical properties of Fe3O4/GO/chitosan composites. Composites Part B: Engineering. 2014;66:89-96.
[14] Ramesh S, Sivasamy A, Rhee KY, Park SJ, Hui D. Preparation and characterization of maleimide–polystyrene/SiO2–Al2O3 hybrid nanocomposites by an in situ sol–gel process and its antimicrobial activity. Composites Part B: Engineering. 2015;75:167-175.
[15] Steven CR, Busby GA, Mather C, Tariq B, Briuglia ML, Lamprou DA, et al. Bioinspired silica as drug delivery systems and their biocompatibility. Journal of Materials Chemistry B. 2014;2:5028.
[16] Kang Y, Chen X, Song S, Yu L, Zhang P. Friction and wear behavior of nanosilica-filled epoxy resin composite coatings. Applied Surface Science. 2012;258:6384-6390.
[17] Chen R, Qu H, Agrawal A, Guo S, Ducheyne P. Controlled release of small molecules from silica xerogel with limited nanoporosity. Journal of materials science Materials in medicine. 2013;24:137-146.
[18] Radin S, El-Bassyouni G, Vresilovic EJ, Schepers E, Ducheyne P. In vivo tissue response to resorbable silica xerogels as controlled-release materials. Biomaterials. 2005;26:1043-1052.
[19] Barbé C, Bartlett J, Kong L, Finnie K, Lin HQ, Larkin M, et al. Silica particles: A novel drug-delivery system. Advanced materials. 2004;16:1959-1966.
[20] Barbé CJ, Kong L, Finnie KS, Calleja S, Hanna JV, Drabarek E, et al. Sol–gel matrices for controlled release: from macro to nano using emulsion polymerisation. Journal of Sol-Gel Science and Technology. 2008;46:393-409.

[21] Soleimani Dorcheh A, Abbasi MH. Silica aerogel; synthesis, properties and characterization. Journal of Materials Processing Technology. 2008;199:10-26.
[22] Zakeri-Milani P, Loveymi BD, Jelvehgari M, Valizadeh H. The characteristics and improved intestinal permeability of vancomycin PLGA-nanoparticles as colloidal drug delivery system. Colloids and Surfaces B: Biointerfaces. 2013;103:174-181.
[23] Shah SR, Henslee AM, Spicer PP, Yokota S, Petrichenko S, Allahabadi S, et al. Effects of antibiotic physicochemical properties on their release kinetics from biodegradable polymer microparticles. Pharmaceutical research. 2014;31:3379-3389.
[24] Loveymi BD, Jelvehgari M, Zakeri-Milani P, Valizadeh H. Design of vancomycin RS-100 nanoparticles in order to increase the intestinal permeability. Advanced pharmaceutical bulletin. 2012;2:43-56.
[25] Kierys A, Rawski M, Goworek J. Polymer–silica composite as a carrier of an active pharmaceutical ingredient. Microporous and Mesoporous Materials. 2014;193:40-46.
[26] Xing Q, Li N, Jiao Y, Chen D, Xu J, Xu Q, et al. Near-infrared light-controlled drug release and cancer therapy with polymer-caged upconversion nanoparticles. RSC Adv. 2015;5:5269-5276.
[27] da Fonseca LS, Silveira RP, Deboni AM, Benvenutti EV, Costa TM, Guterres SS, et al. Nanocapsule@xerogel microparticles containing sodium diclofenac: a new strategy to control the release of drugs. International journal of pharmaceutics. 2008;358:292-295.
[28] Costache MC, Vaughan AD, Qu H, Ducheyne P, Devore DI. Tyrosine-derived polycarbonate-silica xerogel nanocomposites for controlled drug delivery. Acta biomaterialia. 2013;9:6544-6552.
[29] Mora-Huertas CE, Fessi H, Elaissari A. Polymer-based nanocapsules for drug delivery. International journal of pharmaceutics. 2010;385:113-142.
[30] Singh LP, Bhattacharyya SK, Kumar R, Mishra G, Sharma U, Singh G, et al. Sol-Gel processing of silica nanoparticles and their applications. Advances in colloid and interface science. 2014;214C:17-37.
[31] Auliawan A, Woo EM. Crystallization kinetics and degradation of nanocomposites based on ternary blend of poly(L-lactic acid), poly(methyl methacrylate), and poly(ethylene oxide) with two different organoclays. Journal of Applied Polymer Science. 2012;125:E444-E458.
[32] Wu D, Cheng Y, Feng S, Yao Z, Zhang M. Crystallization Behavior of Polylactide/Graphene Composites. Industrial & Engineering Chemistry Research. 2013;52:6731-6739.
[33] Feczkó T, Tóth J, Dósa G, Gyenis J. Influence of process conditions on the mean size of PLGA nanoparticles. Chemical Engineering and Processing: Process Intensification. 2011;50:846-853.
[34] Feczkó T, Tóth J, Dósa G, Gyenis J. Optimization of protein encapsulation in PLGA nanoparticles. Chemical Engineering and Processing: Process Intensification. 2011;50:757-765.
[35] Li J, Su L, Li J, Liu M-F, Chen S-F, Li B, et al. Influence of sucrose on the stability of W1/O/W2 double emulsion droplets. RSC Adv. 2015;5:83089-83095.
[36] Holloway JL, Lowman AM, Palmese GR. Aging behavior of PVA hydrogels for soft tissue applications after in vitro swelling using osmotic pressure solutions. Acta biomaterialia. 2013;9:5013-5021.
[37] Shin M, Kim HK, Lee H. Dopamine-loaded poly(D,L-lactic-co-glycolic acid) microspheres: new strategy for encapsulating small hydrophilic drugs with high efficiency. Biotechnology progress. 2014;30:215-223.
[38] Özalp Y, Özdemir N, Kocagöz S, Hasirci V. Controlled release of vancomycin from biodegradable microcapsules. Journal of microencapsulation. 2001;18:89-110.
[39] Feng S, Nie L, Zou P, Suo J. Effects of drug and polymer molecular weight on drug release from PLGA-mPEG microspheres. Journal of Applied Polymer Science. 2015;132.

[40] Gavini E, Chetoni P, Cossu M, Alvarez MG, Saettone MF, Giunchedi P. PLGA microspheres for the ocular delivery of a peptide drug, vancomycin using emulsification/spray-drying as the preparation method: in vitro/in vivo studies. European journal of pharmaceutics and biopharmaceutics : official journal of Arbeitsgemeinschaft fur Pharmazeutische Verfahrenstechnik eV. 2004;57:207-212.
[41] Xu J, Xu B, Shou D, Xia X, Hu Y. Preparation and Evaluation of Vancomycin-Loaded N-trimethyl Chitosan Nanoparticles. Polymers. 2015;7:1850-1870.

Figures

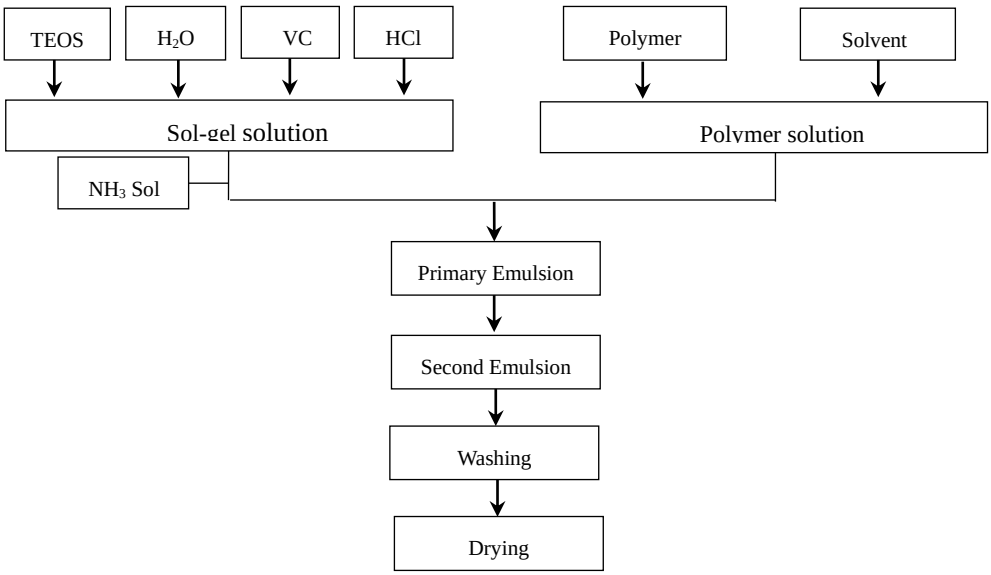

Figure 1 A flow chart for fabrication of nanoparticles in micro-carrier

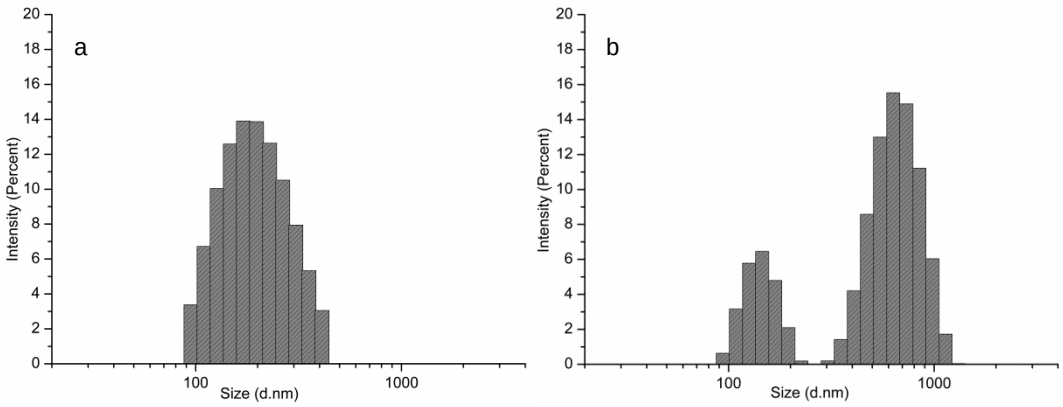

Figure 2 Particle size distribution of samples: (a) the smallest diameter (192 nm) and (b) the biggest diameter (569 nm)

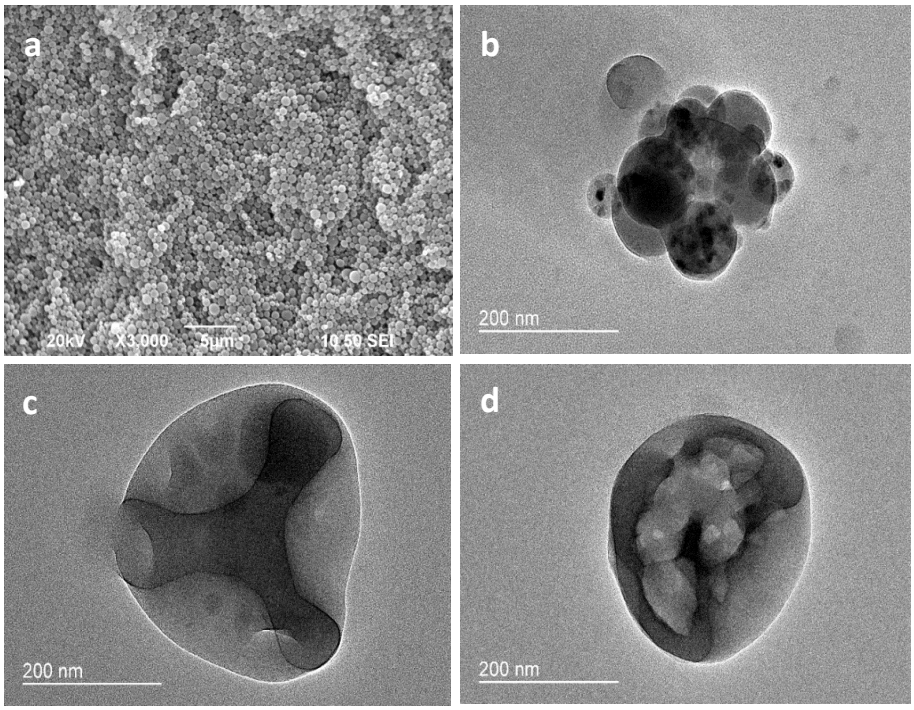

Figure 3 Morphologies of drug loaded composite nanoparticles, (a) SEM and (b-d) TEM images

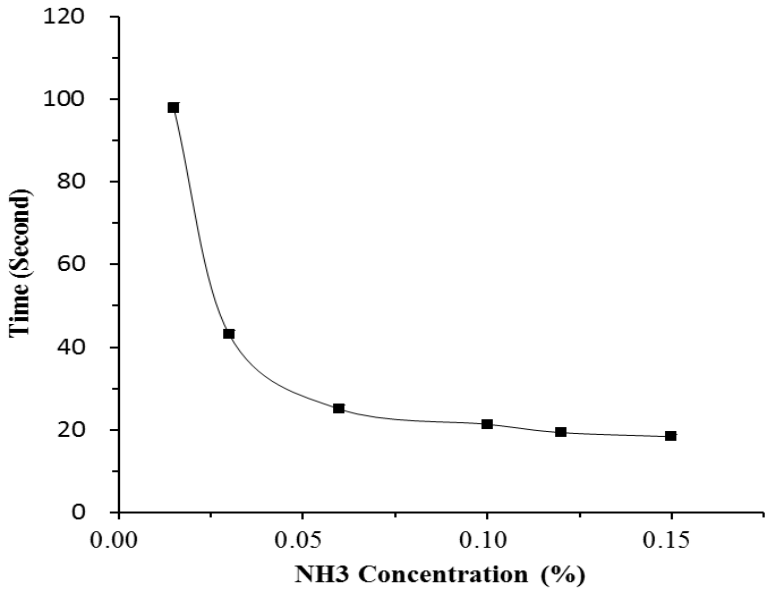

Figure 4 Relationships between NH_3 concentration in sol-gel solution and time required for sol-gel to become gel.

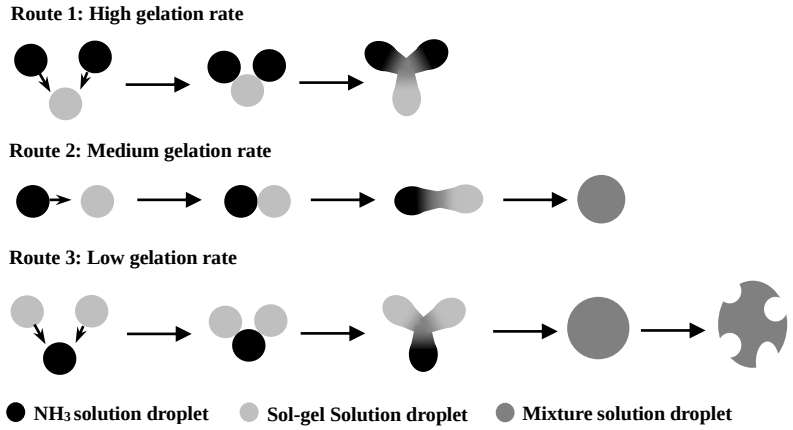

Figure 5 Schematic of possible types of the collisions between NH_3 and sol-gel solution droplets

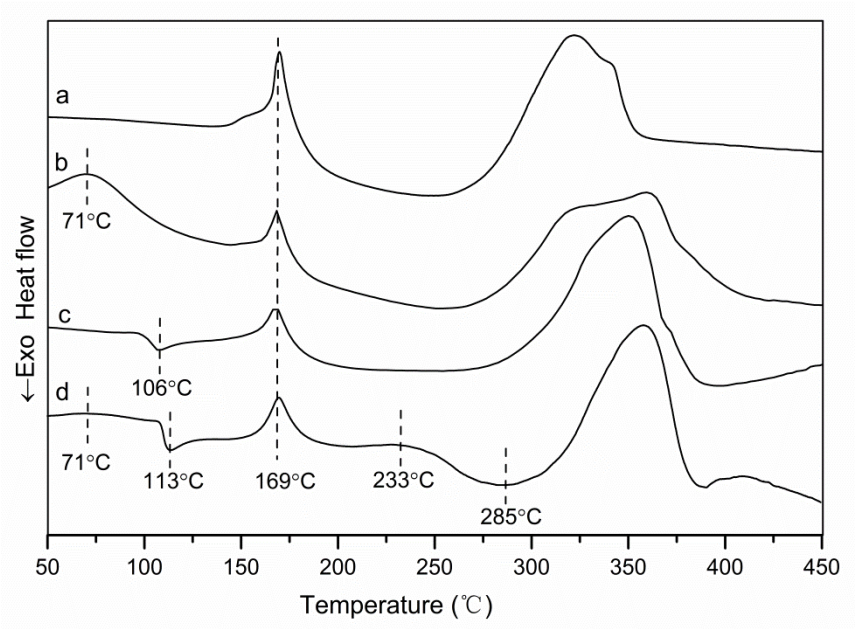

Figure 6 DSC curves of (a) PLA, (b) mixture of all raw materials of drug loaded composite nanoparticles, (c) drug free composite nanoparticles and (d) drug loaded composite nanoparticles

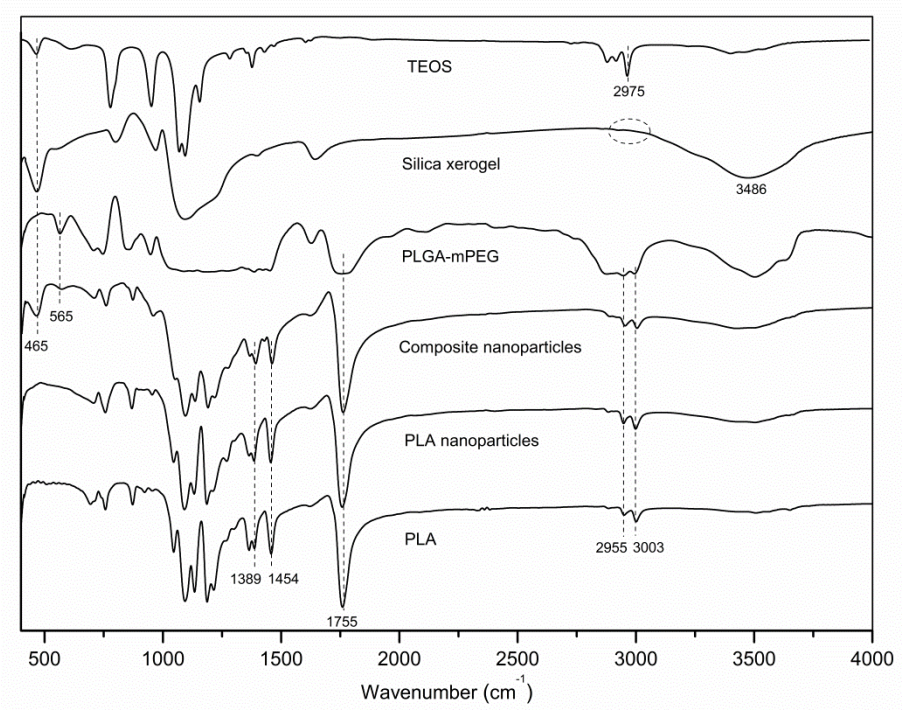

Figure 7 FT-IR spectra of various samples and raw materials

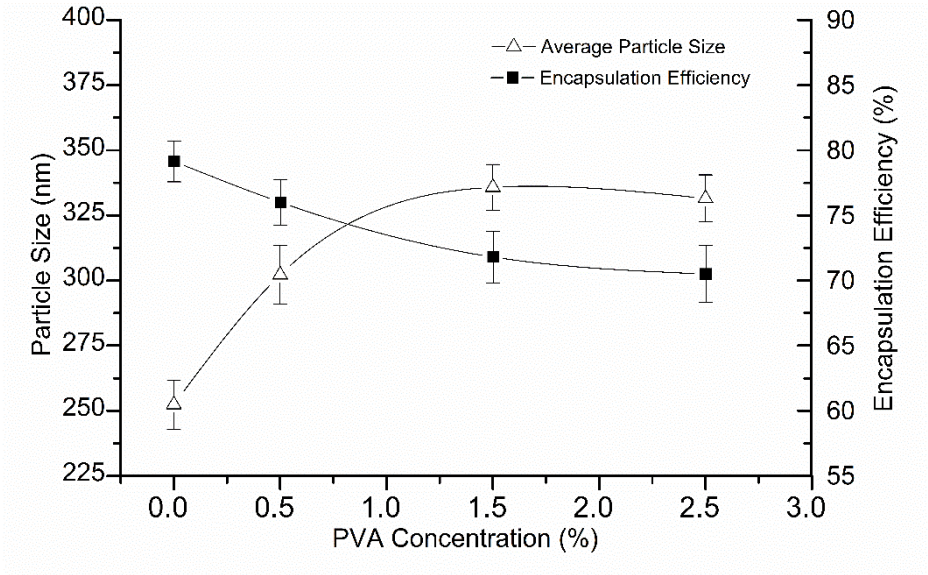

Figure 8 Effect of PVA concentrations on the average diameter and drug encapsulation efficiency of composite nanoparticles (2^{nd} sonication time =1.5 minutes). The error bars represent standard deviation (n=3).

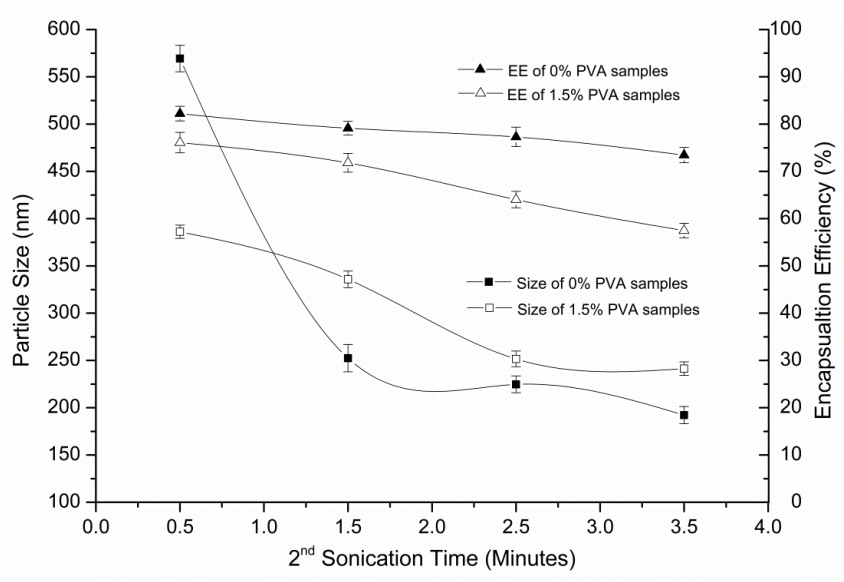

Figure 9 Effect of 2nd sonication time on the average diameter and drug encapsulation efficiency of composite nanoparticles with different PVA Concentrations. The error bars represent standard deviation (n=3).

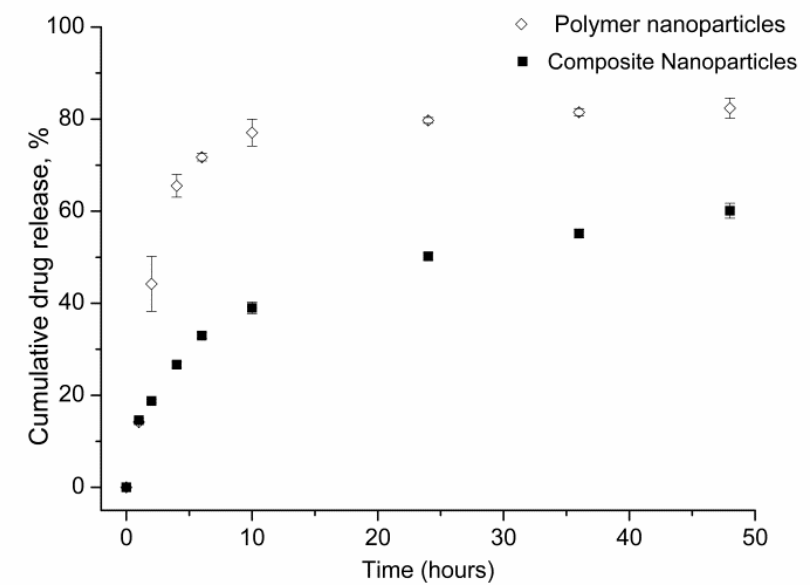

Figure 10 Cumulative release of vancomycin from drug loaded composite nanoparticles and drug loaded polymer nanoparticles as a function of the release time. The error bar represents the standard deviation (n=3).

Table 1 Effects of different roles of PVA

Role	Effect	
	EE	Size
Emulsifier	-*	-
Viscosity enhancer	+*	+
Osmotic pressure solution	-	/

* "+" indicated positive link with PVA concentration;"-" indicated negative link with PVA concentration

Table 2 Comparison of composite nanoparticles with other similar nano/micro particles in literature

Polymer	Size	EE	Burst release (24hr)	Fabrication Techniques	Year	Ref
PLGA	450-466nm	38.4-78.6%	100%	Double emulsion	2013	[22]
PLA	5-15 μm	30.2-74.0%	~20%	Double emulsion	2001	[38]
PLGA-mPEG	6-12μm	29.1-53.5%	~52%	Double emulsion	2014	[39]
PLGA	~11μm	84.0-99.5%	100%	Emulsion/spray drying	2004	[40]
Chitosan	220nm	73.65%	65%	ionic complexation	2015	[41]
PLA/PLGA-mPEG	**192-569nm**	**57.5-82.2%**	**50%**	**Emulsion/sol-gel**	**Current**	**/**

Table 3 Comparison of composite nanoparticles with polymer nanoparticles prepared with similar process condition.

Sample*	Size	EE	Burst release (24hr)	Complete release Time
a	356±9 nm	71.8%	50%	66 days
b	261±7 nm	/	/	/
c	356±6 nm	34.2%	80%	20 days
d	351±3 nm	/	/	/

* (a) drugs loaded composite nanoparticle, (b) drug free composite nanoparticles, (c) drug loaded polymer nanoparticles and (d) drug free polymeric nanoparticles